Vol 17 No 1, January 2008
1674-1056/2008/17(01)/0232-06
Chinese Physics B
© 2008 Chin. Phys. Soc.
and IOP Publishing Ltd

A simple model for approximate bandgap structure calculation of all-solid photonic bandgap fibre based on an array of rings*

Fang Hong(方 宏)†, Lou Shu-Qin(娄淑琴), Guo Tie-Ying(郭铁英),
Yao Lei(姚 磊), Li Hong-Lei(李宏雷), and Jian Shui-Sheng(简水生)

Key Laboratory of All Optical Network & Advanced Telecommunication Network of EMC, Institute of Lightwave Technology, Beijing Jiaotong University, Beijing 100044, *China*

(Received 1 March 2007; revised manuscript received 6 July 2007)

A simple model for approximate bandgap structure calculation of all-solid photonic bandgap fibre based on an array of rings is proposed. In this model calculated are only the potential modes of a unit cell, which is a high-index ring in the low-index background for this fibre, rather than the whole cladding periodic structure based on Bloch's theorem to find the bandgap. Its accuracy is proved by comparing its results with the results obtained by using the accurate full-vector plane-wave method. High speed in computation is its great advantage over the other exact methods, because it only needs to find the roots of one-dimensional analytical expressions. And the results of this model, mode plots, offer an ideal environment to explore the basic properties of photonic bandgap clearly.

Keywords: photonic bandgap fibre; bandgap structure; multi-layer waveguide; plane-wave method
PACC: 4281, 4270Q

1. Introduction

Photonic bandgap fibre (PBGF) is optical fibre in which a low index core is surrounded by photonic crystal cladding with a perfectly periodic structure.[1] Light is confined to the core by the photonic bandgap of the cladding. Among the fibres of this kind, hollow-core PBGF is the most important and attractive, due to its advantages such as high damage threshold,[2] low bending loss,[3] a number of potential applications in all optical sensors in which a high overlap between light and gas or liquid is needed,[4] and so on. However, hollow-core PBGFs have some problems in the fabrication process and connection with other fibres.[5] Furthermore, the detailed bandgap properties of the cladding composed of air-holes and glass are rather complicated conceptually. Advance rather than intuitive leap forward in their design tends to be made through a great number of experiments and a variety of numerical models. Recently, several research groups have focused on a new class of PBGFs called all-solid PBGF, which is formed using the far lower index contrast available from undoped and updoped silica (for example, doped with germanium).[6] It has been demonstrated that all-solid PBGFs can offer a much more palpable environment to explore the basic properties of photonic bandgaps than the hollow core PBGFs. Furthermore, they have exhibited the unusual dispersive characteristics, and a lot of applications including spectral filtering, high-power system and dispersion management.[6−8]

However, these fibres have a larger bend loss than the hollow-core PBGFs. Fortunately, a feasible way to suppress this bend loss has been proved numerically and analytically.[9] According to the numerical results, the bend loss can be suppressed by using an array of rings with high index instead of high index rods in all-solid PBGFs.[10] The transversal cross section of this fibre is shown in Fig.1, where the inner diameter and the outer diameter of rings are denoted by $2a$ and $2b$, respectively, the separation between the centres of two adjacent rings is represented by Λ.

In this paper, we develop a simple model for approximate bandgap structure calculation of all-solid PBGFs based on an array of rings. Through calculating the modes of a unit cell, which is a high-index ring in a low-index background, rather than the whole

*Project supported by the National High Technology Research and Development Program of China (Grant No 2004AA31G200) and Beijing Jiaotong University Foundation, China (Grant No 2005SM002).
†E-mail: macrofang@263.net

cladding periodic structure based on Bloch's theorem, an approximate bandgap structure can be found. In the following section introduced is the principle of the proposed simple model for approximate bandgap structure calculation and also shown are its analytical expressions together with some key process of their deducing. In Section 3 given is a comparison between the results obtained by using the proposed simple model and the full-vector plane-wave method. And then, in the last section presented are some conclusions and discussion about the advantages and the limitations of this simple model.

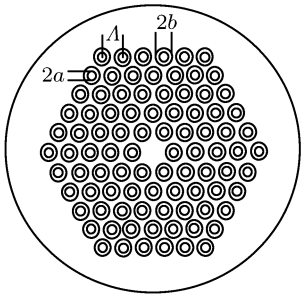


Fig.1. Schematic diagram of the transversal cross section of all-solid photonic bandgap fibre based on an array of rings. The grey annular regions are of Ge-doped high index rings with index step of about one percent, whereas the other regions are of undoped SiO_2.

2. The simple model for approximate bandgap structure calculation

To analyse the properties of PBGFs, the first step is to calculate its bandgap, in which the light cannot escape from the core through the cladding. In other words, the light with spectral wavelengths cannot be guided in the cladding, and the corresponding photonic states do not exist there. Therefore, if we find out all the potential modes in the cladding, the region where the photonic states do not exist, i.e. the location of photonic bandgaps (PBG), can be described. In order to map the plot of the effective index of these modes versus the wavelength or frequency, it is necessary to map the maximal and the minimal effective index lines of each mode. The modes of the cladding with a perfectly periodic structure can be simply solved from the wave equation in a unit cell with two kinds of boundary conditions given by Bloch's theorem.[11] In the case of the fibre shown in Fig.1, a hexagonal cell with a high-index material ring can be employed to represent the unit cell. But it is more difficult to apply the boundary conditions to a hexagonal cell than a square one or a circular one. To simplify the calculation, we employ a circular cell to represent the hexagonal cell approximately. As seen in Fig.2, a hexagonal unit cell containing a central ring is replaced by a circle one whose outer radius is c. The value of c, i.e. $(\sqrt{3}/2\pi)^{1/2}\Lambda$, is determined by keeping equal the area between the original hexagonal cell and the corresponding circle cell. This transform is widely employed in the effective-index method of analysing index-guiding photonic crystal fibres (PCFs).[12,13] The equivalent transform can be used in the case where the value of $2b/\Lambda$ is not very large, and so the corners of the hexagonal cell accounts for an insignificant fraction of the background. In addition, scalar weak-guidance approximation can be used to analyse the properties of fibre as the index contrast between the high-index region and the low-index region is small. Because of the one percent index step, the scalar wave equation can be used to calculate the modes of the multi-layer optical waveguide shown in Fig.2.

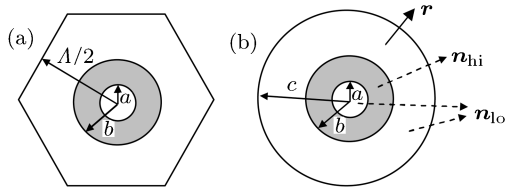


Fig.2. A hexagonal unit cell (a) and its corresponding circular unit cell (b), where the white regions are the low-index regions, and the grey regions are the high-index regions with an index step of about one percent.

Considering the characteristics of each kind of Bessel function and the three-layer optical waveguide shown in Fig.2(b), we can deduce the general solutions of the scalar wave equation within each layer as listed below:

$$\Psi(r)=\begin{cases} r<a, & \begin{cases} I_L(Wr), & \text{for } \beta>kn_{\rm lo}, \quad (1)\\ J_L(Qr), & \text{for } \beta<kn_{\rm lo}, \quad (2)\end{cases}\\ a<r<b, & AJ_L(Ur)+BN_L(Ur), \quad (3)\\ b<r<c, & \begin{cases} CK_L(Wr)+DI_L(Wr), & \text{for } \beta>kn_{\rm lo}, \quad (4)\\ EJ_L(Qr)+FN_L(Qr), & \text{for } \beta<kn_{\rm lo}, \quad (5)\end{cases}\end{cases}$$

where I_L, J_L, N_L, and K_L are L order Bessel functions; A, B, C, D, E, and F are unknown constants; β is the propagation constant, which is derived from the expression $E(x,y,z)=e(x,y)\mathrm{e}^{\mathrm{j}\beta z}$ with $E(x,y,z)$ being the electric field of a mode, and $e(x,y)$ being its transverse distribution; k is the free space wave number; U, W and Q are the familiar parameters of optical waveguide theory,[14] and they are $U=\sqrt{k^2n_{\rm hi}^2-\beta^2}$, $W=\sqrt{\beta^2-k^2n_{\rm lo}^2}$, $Q=\sqrt{k^2n_{\rm lo}^2-\beta^2}$, and $\beta<kn_{\rm hi}$.

According to the Maxwell's equations, the field distributions Ψ and Ψ' are continuous at the interface between two different materials.[14] Using the boundary condition at $r=a$, we acquire the following Eqs.(6) and (7) for $\beta>kn_{\rm lo}$ and $\beta<kn_{\rm lo}$, respectively:

$$\begin{cases} AJ_L(Ua)+BN_L(Ua)=I_L(Wa),\\ U[AJ_L'(Ua)+BN_L'(Ua)]=WI_L'(Wa),\end{cases} \quad \beta>kn_{\rm lo}, \tag{6}$$

$$\begin{cases} AJ_L(Ua)+BN_L(Ua)=J_L(Qa),\\ U[AJ_L'(Ua)+BN_L'(Ua)]=QJ_L'(Qa),\end{cases} \quad \beta<kn_{\rm lo}. \tag{7}$$

Coefficients A and B can be obtained from Eqs.(6) and (7), they are represented by the following Eqs.(8) and (9):

$$\begin{cases} A=UN_{L+1}(Ua)I_L(Wa)+WI_{L+1}(Wa)N_L(Ua),\\ B=UI_L(Wa)J_{L+1}(Ua)+WJ_L(Ua)I_{L+1}(Wa),\end{cases} \quad \beta>kn_{\rm lo}, \tag{8}$$

$$\begin{cases} A=UN_{L+1}(Ua)J_L(Qa)-QJ_{L+1}(Qa)N_L(Ua),\\ B=UJ_L(Qa)J_{L+1}(Ua)-QJ_L(Ua)J_{L+1}(Qa),\end{cases} \quad \beta<kn_{\rm lo}. \tag{9}$$

Similarly, by using the boundary condition at $r=b$ we determine the coefficients C, D, E, and F. To shorten the length of article, here we show the results directly as follows:

$$\begin{cases} C=A[WJ_L(Ub)I_{L+1}(Wb)+UJ_{L+1}(Ub)I_L(Wb)]\\ \quad +B[WN_L(Ub)I_{L+1}(Wb)+UN_{L+1}(Ub)I_L(Wb)],\\ D=A[WJ_L(Ub)K_{L+1}(Wb)-UJ_{L+1}(Ub)K_L(Wb)]\\ \quad +B[WN_L(Ub)K_{L+1}(Wb)-UN_{L+1}(Ub)K_L(Wb)],\end{cases} \quad \beta>kn_{\rm lo}, \tag{10}$$

where, A and B take the values in Eq.(8);

$$\begin{cases} E=A[QJ_L(Ub)N_{L+1}(Qb)-UJ_{L+1}(Ub)N_L(Qb)]\\ \quad +B[QN_L(Ub)N_{L+1}(Qb)-UN_{L+1}(Ub)N_L(Qb)],\\ F=A[QJ_L(Ub)J_{L+1}(Qb)-UJ_{L+1}(Ub)J_L(Qb)]\\ \quad +B[QN_L(Ub)J_{L+1}(Qb)-UN_{L+1}(Ub)J_L(Qb)],\end{cases} \quad \beta<kn_{\rm lo}, \tag{11}$$

where, A and B take the values in Eq.(9).

Then, by using the boundary condition at $r = c$, the eigen equations can be deduced. According to the band theory of solid[11,15] and the optical waveguide theory,[14] there exist two kinds of special boundary conditions. One is the condition $\Psi'(c)= 0$, which determines the states with lines of mirror symmetry along the cell boundaries, and these states are the most bonded states of the band with the least spatial field variation, and so they have the highest β. The other is the condition $\Psi(c)= 0$, which determines the states where the cell boundaries are anti-mirror lines, and these states are the most anti-bonded states with the greatest field variation, and so they have the lowest β. Therefore, by using these two kinds of boundary conditions, we can calculate the maximal and minimal effective indices for each potential mode. And then linking the points for different frequencies, we can obtain two lines for each mode, which are called top line and bottom line correspondingly.

So, analytical expressions are obtained as follows: 1) For the top line (the maximal effective index): $\Psi'(c) = 0$

$$\begin{cases} [CK'_L(Wc) + DI'_L(Wc)]W = 0, & \beta > kn_{\rm lo}, \\ [EJ'_L(Qc) + FN'_L(Qc)]Q = 0, & \beta < kn_{\rm lo}; \end{cases} \tag{12}$$

2) For the bottom line (the minimal effective index): $\Psi(c) = 0$

$$\begin{cases} CK_L(Wc) + DI_L(Wc) = 0, & \beta > kn_{\rm lo}, \\ EJ_L(Qc) + FN_L(Qc) = 0, & \beta < kn_{\rm lo}, \end{cases} \tag{13}$$

where L is the azimuthal variation, and it can be any nonnegative integer. Then substitute U, W, Q and the coefficients with their definition and result above, and use $\beta = kn_{\rm eff}$, where $n_{\rm eff}$ is the effective index, then these expressions will have only one unknown $n_{\rm eff}$ at a certain frequency, so finding the roots is very efficient. For each value of L, there are many roots for one equation, numbered by parameter m. So each mode is marked by two parameters (L and m), which is the same as scalar mode LP_{Lm} in the weak-guidance approximation.[14]

Now, we have acquired the top line and bottom line for each potential mode in the cladding, and the region between these two lines is filled with the potential modes for any other boundary condition. Therefore, we can also find out the regions where there is not any potential mode, which are just the bandgaps of cladding.

3. Comparison with plane-wave method

The results of bandgap structure calculated by using the above model are compared with the accurate numerical results calculated with the full-vector plane-wave method.[16,17] Choosing the same parameters as those in Ref.[10], i.e. $n_{\rm hi}$=1.47288, $n_{\rm lo}$=1.457, and b/Λ=0.35, Fig.3 shows the bandgaps of perfectly periodic structure, calculated by using the plane-wave method, and the regions where there are scalar modes of unit cell, calculated by the above model for various inner radii between a=0 (i.e. rod) and a maximum of a/b=0.6. Using the PC with 2.5GHz CPU and 768Mbit memory, it takes more than 3h to map one bandgap plot by using the plane-wave method, whereas it just takes 5 min to map all the potential modes in the same frequency range by the proposed simple model.

All the potential modes in this frequency range have been mapped by the symbol LP_{Lm} in Figs.3(b), (d), (f), and (h). Numerical results exhibit that there are some parts of overlapped region between some modes. And the regions where there is not any potential mode in the mode plot by using the simple model are just the bandgap regions which are consistent with the results by using the plane-wave method, which proves that the proposed simple model can find out the bandgaps of perfectly periodic structure within an acceptable accuracy. In addition, in each plot of Fig.3, there is a cutoff line indicated by a dotted line. In our case, this line is at $n_{\rm eff}$=1.457, which is equal to the index of effective core of the fibre shown in Fig.1. To realize the cladding structure that exhibits PBG covering, the cutoff line is basic requirement for low-index guiding PBGFs.

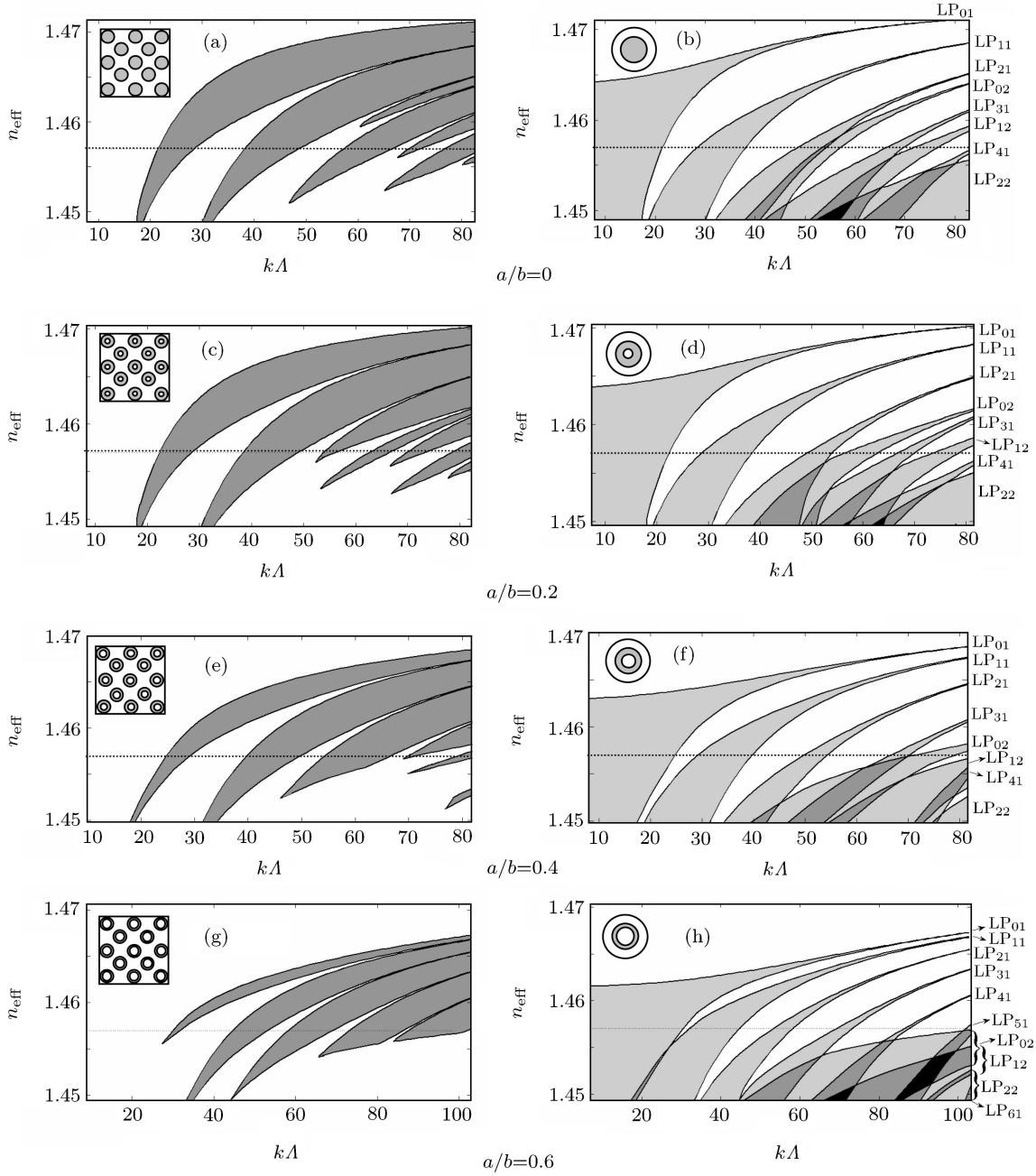


Fig.3. Bandgaps of perfectly periodic structure, calculated by the plane-wave method (a), (c), (e), and (g), and potential scalar mode regions of individual cell, calculated by the proposed simple model (b), (d), (f), and (h) at a/b=0, 0.2, 0.4, and 0.6, respectively.

According to Ref.[9], the fibre bend loss is especially high when the bandgaps are located on their high-frequency edge by an L=0 mode. The reason for that is that L=0 modes are intrinsically more strongly coupled together than $L > 0$ modes. However, for instance, when a=0, i.e. with an array of rods in cladding, the third bandgap is located on its high-frequency edge by LP_{02} mode, so the defect mode in this bandgap will suffer a very large bend loss. When the array of rods is replaced by an array of rings, with the increase of a/b all the modes shift toward lower effective indices and higher frequencies. But the $m > 1$ modes shift much faster than the m=1 modes. Figure 4 shows the LP_{02} mode at different values of a/b. As seen in the figure, the LP_{02} mode shifts toward the region under the cutoff line when a/b =0.6. Now the third bandgap is located on its high-frequency edge by LP_{31} mode as shown in Fig.3(h). Moreover, all of the bandgaps in this frequency range are located on its high-frequency edge by $L > 0$ modes when they cross

the cutoff line. This is the reason why the structure with an array of rings can suppress the bend loss of all-solid PBGFs. On the other hand, the prominent advantage of mode plot for analysing basic properties of bandgaps is exhibited.

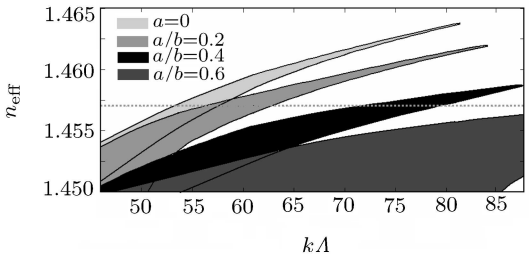


Fig.4. The LP_{02} mode at different values of a/b. The cutoff line is indicated by a dotted line.

4. Conclusions and discussion

In this paper, a simple model for the approximate bandgap structure calculation of all-solid photonic bandgap fibre based on an array of rings is proposed. Its accuracy is proved by comparing its results with the results obtained by using the accurate full-vector plane-wave method. Its high efficiency is the most prominent advantage over the other exact methods, because of its requirement only for finding the roots of one-dimensional analytical expressions. So, it is very useful in the prophase of designing the fibre where the speed of calculation is more important than the accuracy. However, because of two approximations, i.e. replacing the hexagonal unit cell with a circular one and scalar weak-guidance approximation, this simple model has two limitations: b/Λ cannot be too big, and the index contrast between the two materials must be very low. For the former, we find when $b/\Lambda > 0.4$, the simple model will become less accurate because the corners of hexagonal cell exert a more significant influence on the bandgap structure. So, we need to use a more appropriate but complicated boundary condition in calculation. And for the latter, a vector model developed through a similar procedure may be used to cope with the problem. These are the next subjects of our study on PBGFs.

References

[1] Russell P 2003 *Science* **299** 358
[2] Shephard J D, Jones J D C, Hand D P, Bouwmans G, Knight J C, Russell P and Mangan B J 2004 *Opt. Express* **12** 717
[3] Bouwmans G, Luan F, Knight J C, Russell P, Farr L, Mangan B J and Sabert H 2003 *Opt. Express* **11** 1613
[4] Benabid F, Couny F, Knight J C, Birks T A and Russell P 2005 *Nature* **434** 488
[5] Xiao L M, Jin W, Demokan M S, Ho H L, Hoo Y L and Zhao C L 2005 *Opt. Express* **13** 9014
[6] Bouwmans G, Bigot L, Quiquempois Y, Lopez F, Provino L and Douay M 2005 *Opt. Express* **13** 8452
[7] Wang A, George A K and Knight J C 2006 *Opt. Lett.* **31** 1388
[8] Nielsen C K, Jespersen K G and Keiding S R 2006 *Opt. Express* **14** 6063
[9] Birks T A, Luan F, Pearce G J, Wang A, Knight J C and Bird D M 2006 *Opt. Express* **12** 5688
[10] Stone J M, Pearce G J, Luan F, Birks T A, Knight J C, George A K and Bird D M 2006 *Opt. Express* **14** 6291
[11] Burns G 1985 *Solid State Physics* (Orlando, Fla.: Academic Pr. Inc.) p252
[12] Li S G, Liu X D and Hou L T 2003 *Acta Phys. Sin.* **52** 2811 (in Chinese)
[13] Zhao X T, Hou L T, Liu Z L, Wang W, Wei H Y and Ma J R 2007 *Acta Phys. Sin.* **56** 2275 (in Chinese)
[14] Snyder A W and Love J D 1983 *Optical Waveguide Theory* (London, New York: Chapman and Hall) p640
[15] Guan S Q, Wang Z G and Zhao X G 2003 *Chin. Phys.* **12** 899
[16] Guo S P and Albin S 2003 *Opt. Express* **11** 167
[17] Wang J L and Chen H M 2007 *Acta Phys. Sin.* **56** 922 (in Chinese)